ARTICLE

Ag−TiO_2 Nanoparticle Codoped SiO_2 Films on ZrO_2 Barrier-Coated Glass Substrates with Antibacterial Activity in Ambient Condition

Anindita Mukhopadhyay,[†] Sujit Basak,[‡] Jugal Kishore Das,[†] Samar Kumar Medda,[†] Krishnananda Chattopadhyay,[‡] and Goutam De*[,†]

Nano-Structured Materials Division, Central Glass and Ceramic Research Institute, 196 Raja S. C. Mullick Road, Kolkata 700032, India, and Structural Biology and Bioinformatics Division, Indian Institute of Chemical Biology, 4 Raja S. C. Mullick Road, Kolkata 700032, India

ABSTRACT Anatase TiO_2 and Ag nanoparticles (NPs) codoped SiO_2 films were prepared by the sol−gel method. Proportionate amounts of 3-(glycidoxypropyl)trimethoxysilane (GLYMO), tetraethylorthosilicate (TEOS) and 3-(methacryloxypropyl)trimethoxysilane (MEMO) derived inorganic−organic silica sol, commercially available dispersed anatase TiO_2 NPs, and $AgNO_3$ were used to prepare the sols. The films were prepared on ZrO_2 (cubic) precoated soda-lime glass substrates by a single-dipping technique and heat-treated at 450 °C in air and H_2/Ar atmosphere to obtain hard, relatively porous, and transparent coatings of thickness >600 nm. The ZrO_2 barrier layer was previously applied on soda-lime glass to restrict the diffusion of Ag into the substrate. The Ag−TiO_2 NPs incorporated SiO_2 films were intense yellow in color and found to be fairly stable at ambient condition for several days under fluorescent light. These films show a considerable growth inhibition on contact with the gram negative bacteria *E. coli*.

KEYWORDS: Ag-TiO_2 NPs codoped SiO_2 film • anatase TiO_2 • sol−gel • antibacterial activity • cubic ZrO_2 barrier film on glass

1. INTRODUCTION

Silver is so far one of the best known antimicrobial/antifungal agent due to a strong cytotoxic effect toward a broad range of micro organism, and more so because of its remarkably low human toxicity compared to other heavy metal ions. The antibacterial activity of silver is known to be due to Ag^+ ion, which strongly binds the thiol groups present in the bacterial/microbial cell membrane and thus destroys the cell by rupturing the wall (1). Recently, it has been known that Ag NPs also possess considerable antimicrobial activity (2−10). The antibacterial mechanism of Ag NPs is also assumed to be related to the membrane damage due to free radicals that are derived from the surface of the NPs (4). The potential benefits of nano Ag materials have been recognized even by many industries not only due to their strong antimicrobial activity toward a broad spectrum of bacterial, virus and fungi, but also because of the low rate of development of resistance, which is a common problem in case of commercial antibiotics (11). Because of these unique characteristics, nano silver materials have been used in variety of medical applications and even as biomedical materials like bone cement, artificial skin etc., as well as in the prevention of bacterial/fungal infection related to the use of medical devices (12).

We have been working on the development of sol−gel derived coatings on glass and plastic substrates (13−15). It would be a good idea if Ag NP doped relatively porous coatings can be applied on glass or related substrates for the application of bactericidal/fungicidal applications. It is known that Ag ions can be easily migrated from the glassy SiO_2 coatings toward the glass substrates by the Ag^+/Na^+ exchange reactions (16−18), and for this reason the concentration of doped Ag decreased significantly in the films. So a suitable barrier layer could be useful to prevent the migration of Ag into the glass substrate. We observed that the Ag NPs gradually oxidized (when embedded in sol−gel-derived glassy silica films) with time and the resulting ionic Ag migrated toward the surface and eventually escaped out (19). This could be severe if the coating matrix becomes porous. For this reason, addition of a codopant (e.g., anatase TiO_2 NPs) that can help stabilizing the metallic Ag NPs as well as improve the overall antibacterial property of the coatings would be interesting from application point of view. A few earlier reports on Ag-doped films (20−22) may be highlighted in this context. Jean et al. (20) reported Ag-doped SiO_2 films on microscopic glass following a similar technique reported by us (15). In that work, they observed migration of Ag toward the surface with increasing the annealing temperature from 300 to 600 °C causing formation of colonies of large Ag metal clusters of various size ranges up to micrometer level. As a result, inhomogeneous distribution of large Ag clusters was resulted on the top surface. EDX analysis confirmed presence of very less amount of Ag in the areas out side the Ag colonies, whereas large clusters visible in the colonies contained high amount of Ag. Never-

* Corresponding author. Fax: 91-33-24730957. E-mail: gde@cgcri.res.in.
Received for review April 26, 2010 and accepted August 9, 2010
[†] Central Glass and Ceramic Research Institute.
[‡] Indian Institute of Chemical Biology.
DOI: 10.1021/am100363d

Published on Web 08/18/2010

theless they found good antibacterial performance due to the presence of such Ag clusters. Page et al. (21) reported sol−gel synthesis of Ag_2O–TiO_2 films on microscopic slides (soda-lime glass) and studied their antimicrobial properties after irradiated by UV light (365 nm). Although they incorporated 10 mol % Ag in TiO_2 matrix, only less than 1 at % Ag was found to be present in the final heat-treated coatings. This result confirmed loss of major amount (>90 %) of doped Ag from the coatings. It is expected that a part of Ag was diffused into the glass substrate by Ag^+/Na^+ ion exchange and another part possibly migrated toward the top surface and expelled out of the coating. Another work reported by Shah et al. (22) where Ag salt was impregnated into the hybrid PEG−PU−TiO_2 films of thickness 0.3 mm (prepared by solution casting in a glass Petri dish) followed by UV photo reduction of Ag ions to Ag NPs. The authors reported that the Ag−TiO_2 codoped hybrid film discs showed better antibacterial properties and the Ag NPs are mainly responsible for this.

In this work, we have planned to prepare Ag−TiO_2 NPs incorporated in relatively porous SiO_2 films on ZrO_2 barrier-coated glass substrates. It is known that surface of soda-lime glass can be protected from alkali attack after application of ZrO_2 layer (23). The diffusion of Ag ions is expected to be inhibited because of larger size of Zr atom. The incorporation of anatase TiO_2 may act as a stabilizing agent of metallic Ag NPs, because the later can trap the photogenerated electrons from TiO_2 NPs. Anatase TiO_2 can also enhance the antibacterial activities of Ag NPs (22, 24, 25). So these combined Ag−TiO_2 NPs incorporated relatively porous SiO_2 films with smooth, durable and homogeneous colorful appearance could find important applications in hospitals and other areas where antibacterial coatings on glass or similar substrates are necessary. In this work, we report synthesis of scratch-resistant and brightly yellow colored transparent thin films on glass showing considerable growth inhibition of *E. coli* on contact.

2. EXPERIMENTAL SECTION

2.1. Materials. All chemicals and solvents were used as received. Tetraethylorthosilicate (TEOS), 3-(glycidoxypropyl)-trimethoxysilane (GLYMO), Aluminum acetylacetonate and Zirconium tetraisopropoxide (ZTIP) were supplied by Sigma-Aldrich. 3-(Methacryloxypropyl)trimethoxysilane (MEMO) and anatase suspension (20 wt % anatase TiO_2 in isopropanol; average size of TiO_2 NPs, 15 nm) were obtained from Alfa-Aesar and Nanostructured & Amorphous Materials Inc., respectively. $AgNO_3$ was supplied by Qualigens Chemicals. The solvents and acids used in this work were supplied by Ranchem, India. Millipore water (18.2 MΩ) was used.

2.2. Synthesis of ZrO_2 Sol. Zirconia (2.75 equivalent wt % ZrO_2) sol was prepared by hydrolysis−condensation reaction of Zr tetraisopropoxide (ZTIP) modified with acetylacetone (acac). For this purpose, ZTIP (1 mol) was first reacted with acac (0.5 mol) followed by hydrolysis with water (2 mol) in presence of catalytic amount of HNO_3 (1.1×10^{-3} mol). Isoropanol was used as solvent. This sol was used to prepare the barrier layer on soda-lime glass.

2.3. Synthesis of SiO_2 Sol. Fifteen equivalent weight percent silica (SiO_2) sol was first prepared by cohydrolyzing TEOS and GLYMO (7:3 molar ratio) in n-butanol. The detailed method is described in our previous paper (14).

Table 1. Nominal Compositions (mol %) of the Main Precursors Used to Prepare the TiO_2 NPs Incorporated SiO_2 (TiO_2−SiO_2) and Ag−TiO_2 NPs Incorporated SiO_2 (Ag−TiO_2−SiO_2) Sols

precursor	TiO_2−SiO_2 (mol %)	Ag−TiO_2−SiO_2 (mol %)
GLYMO	35	33.25
TEOS	15	14.25
MEMO	10	9.5
anatase TiO_2	40	38
$AgNO_3$		5

2.4. Synthesis of TiO_2−SiO_2 Sol. Appropriate amounts (in grams) of GLYMO (6.41×10^{-2} mol) and TEOS (2.74×10^{-2} mol) were first stirred in n-butanol. Water (1.37×10^{-1} mol) and a catalytic amount of 1N HNO_3 (0.88×10^{-4} mol) were dissolved in n-propanol and added to the above mixture and stirred for 30 min. The sol was then refluxed at 78−79 °C for 1.5 h and cooled at room temperature. MEMO (1.83×10^{-2} mol) was then added and the mixture was stirred for another 30 min. At this stage, a calculated amount of anatase dispersion (7.31×10^{-2} mol with respect to equivalent TiO_2) was added slowly with constant stirring. A water (6.59×10^{-2} mol)/1-propanol mixture was then added and the reaction mixture was stirred for another 45 min. To this faint yellow colored clear sol, solid Al(acac)$_3$ was added (1.28×10^{-3} mol) with stirring. Overall 15 equivalent oxide wt % ($SiO_2 + TiO_2$) was maintained by adding calculated amount of 1-butanol. The SiO_2/TiO_2 molar ratio was maintained at 60/40. The mol ratios of the main components used to prepare this sol are given in Table 1. This TiO_2 NPs incorporated SiO_2 sol (designated as TiO_2−SiO_2) was filtered twice using Whatman no. 1 filter paper and kept for 36 h for aging before use.

2.5. Ag Doping. Five mol % Ag (with respect to the SiO_2 or (TiO_2 and SiO_2)) was doped into the SiO_2 and TiO_2−SiO_2 sols by adding calculated amount of $AgNO_3$ dissolved in minimum amount of water (Table 1). The doped sol was stirred for 15 min prior to use for coating preparation.

2.6. Preparation of Films. Prior to film deposition the soda-lime glass slides were cleaned with a warm neutral detergent solution, rinsed with distilled water and isopropanol, and finally, boiled in isopropanol for 5 min. The films were prepared using a single dipping technique (Dip-master 200, Chemat Corporation). For the deposition of the barrier layer, the cleaned soda-lime glass slides were first coated with the 2.75 wt % ZrO_2 sol with a withdrawal velocity of 13 cm min^{-1} followed by drying at 60 °C (1 h) and finally heating at 500 °C with a holding time of 1 h. These barrier-coated slides were then used to deposit films using undoped and Ag-doped SiO_2 and TiO_2−SiO_2 sols. A withdrawal velocity of 9.5 cm min^{-1} was maintained to deposit such films. These films were dried at 60 °C for 1 h and 95 °C for 1.5 h followed by heat-treated at 450 °C (ramp 2 °C min^{-1}) in air with a holding time of 1 h at the final temperature. The Ag-doped films were finally heat-treated at 450 °C in 10% H_2 (v/v)-balance Ar (hence forth will be designated as H_2/Ar) gas atmosphere for 1 h. The films (without Ag) were also prepared on one-side-polished Si wafers following the identical preparative conditions as stated above for the measurement of refractive index values.

2.7. Antibacterial Studies of the Films with *E. coli* Bacteria. For the antibacterial studies, nutrient agar media (Luria Broth, LB) was prepared in water by mixing tryptone, NaCl, agarose gel powder, and yeast extract in the amount of 1, 0.5, 1.5, and 0.5% respectively, with respect to the total volume of media. The mixture was taken in a conical flask and autoclaved for 45 min at 120 °C. The conical flask was kept in

room temperature for 2 h for cooling and then poured into separate Petri dishes. For bacterial culture, about 1 in. × 1 in. film samples were cut from the coated part of the respective samples and used. The surface of all the film samples were cleaned with absolute ethanol soaked tissue paper prior to antibacterial test. Samples were placed in separate Petri dishes on top of the predeposited LB. A clean soda-lime glass piece was used as a control sample. After placing the film samples, a thin layer of LB was further deposited on top. These plates were kept for 1 h for complete gelation of the agar and after that a solution of *E. coli* was evenly spread over the each gel plate in the respective Petri dishes. Two sets of plates were incubated at 37 °C in the humid chamber to develop the bacterial colonies. One set of plates was taken out at different time intervals to monitor the bacterial growth kinetics. In a separate experiment, the plates were incubated sufficiently long time to allow the completion of the bacterial growth (24 h). The bacterial colonies formed in each plate were observed and photographed for comparison.

2.8. Film Characterization. The top surface of the films deposited on barrier-coated soda-lime glass slides was first cleaned with ethanol or isopropanol soaked tissue paper and used for different characterizations as mentioned below. The UV−visible spectra of the films were recorded by a Cary50 scan (Varian) spectrometer with baseline correction in air. The thickness and refractive index measurements of the films deposited on Si wafer were done using a J. A. Woollam Co. M2000 spectroscopic ellipsometer. Thickness of the films deposited on glass substrates were also measured with a profilometer (Surfcorder SE-2300). X-ray diffraction (XRD) patterns of the films were recorded with a Rigaku SmartLab X-ray diffractometer operating at 9 kW (200 mA × 45 kV) using Cu Kα (λ = 1.5406 Å) radiation. A grazing incidence angle of 0.3° was used to record the XRD patterns of the films. Field emission scanning electron microscopy (FESEM) was done using a ZEISS SUPPRA 35VP microscope to observe the surface of the film. Transmission electron microscopy (TEM) measurements were carried out with a Tecnai G^2 30ST (FEI) operating at 300 kV. For this purpose, cleaned film was scratched carefully and the scratched off film samples was placed on a carbon-coated copper grid for TEM study.

3. RESULTS AND DISCUSSION

3.1. General. Inorganic−organic hybrid silica sols (derived from GLYMO and TEOS) were used to prepare the host SiO_2 matrix because this approach yielded relatively thicker, transparent and hard coatings by a single dipping technique. In this method, GLYMO−TEOS were cohydrolyzed and coatings were prepared and cured at 95 °C. The curing agent $Al(acac)_3$ added in the sol helped to polymerize the GLYMO originated epoxy groups to polyethylene oxide, and as a result the film became hard at 95 °C. These coatings became slightly porous (26) after the heat-treatment at 450 °C because of the decomposition and removal of a high amount of covalently bonded organic groups attached with silicon (Si−CH_2−CH_2−O−). When high amount of TiO_2 NPs (40 equiv mol %) was introduced into the above GLYMO−TEOS-derived SiO_2 sol, white precipitation started to form and the sol became nontransparent. However, addition of MEMO into the GLYMO−TEOS-derived sol prior to the addition of TiO_2 dispersion, followed by second step hydrolysis−condensation reactions yielded a stable, almost transparent and homogeneous sol suitable for depositing good-quality films. It seemed that the MEMO originated methacryloxy groups helped in stabilizing the TiO_2 NPs in the sol.

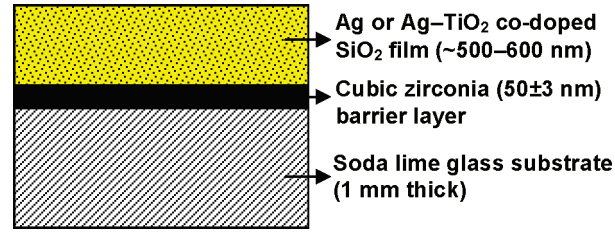

FIGURE 1. Schematic diagram showing the film layers.

Table 2. Thickness and Refractive Index Values of the Films Heat-Treated at 450 °C

film[a]	thickness (nm)	refractive index[b]
SiO_2	510 ± 10	1.412 ± 0.005
TiO_2−SiO_2 (40:60)	640 ± 10	1.510 ± 0.005

[a] Films were deposited on one side polished Si wafer. [b] Values are reported at the wavelength of 633 nm.

As one of our main goals is to restrict the diffusion of Ag into the soda-lime glass substrates, all films were deposited on ZrO_2 barrier-coated substrates. Design of the film assemblies is shown schematically in Figure 1. The ZrO_2 films deposited on soda-lime substrates were heat-treated at 500 °C to obtain a crystalline ZrO_2 film of thickness 50 ± 3 nm. These ZrO_2 barrier-coated substrates were used to deposit Ag, TiO_2, and Ag-TiO_2 codoped SiO_2 films. The heat-treated (450 °C/1 h in air) SiO_2 and TiO_2 NPs incorporated SiO_2 (TiO_2:SiO_2 = 40:60) films (without Ag) deposited on ZrO_2 barrier-coated substrates were visually transparent and homogeneous. Thickness and refractive index (RI) values of these films are given in Table 2. SiO_2 and TiO_2−SiO_2 films showed RI values of 1.412 ± 0.005 and 1.510 ± 0.005 (Table 2), respectively, which are lower than the expected values of SiO_2 (1.458) and TiO_2−SiO_2 (1.872), indicating existence of porosity in these films. In the latter case (TiO_2−SiO_2), more porosity is expected because the difference of RI values is relatively higher. The surface hardness of final heat-treated TiO_2 NPs incorporated SiO_2 (TiO_2−SiO_2) and Ag−TiO_2 codoped SiO_2 was found to be ∼5H (pencil hardness as per ASTM D3363), which is quite good for any practical applications. The Ag-doped films were first dried at 95 °C, and during this drying period Ag ions were reduced to Ag NPs, as well as GLYMO-originated epoxy groups were polymerized to polyethylene oxides (14). The formation of Ag NPs during the drying time was helpful because metallic Ag would not be able to migrate at the early stages. The dried (95 °C) Ag and Ag−TiO_2 codoped SiO_2 films were yellow in color and transformed to colorless after heat-treatment at 450 °C in air, and then turned to bright yellow when reheated at 450 °C in a H_2/Ar atmosphere. The heat-treated Ag-TiO_2 codoped films appeared homogeneous and spot-free and can be cleaned with water and organic solvents (isopropanol, ethanol and acetone) without any surface damage. These films remained stable at ambient condition (no color fading was observed when kept under room light up to 45 days) and can be stored (wrapped with paper in

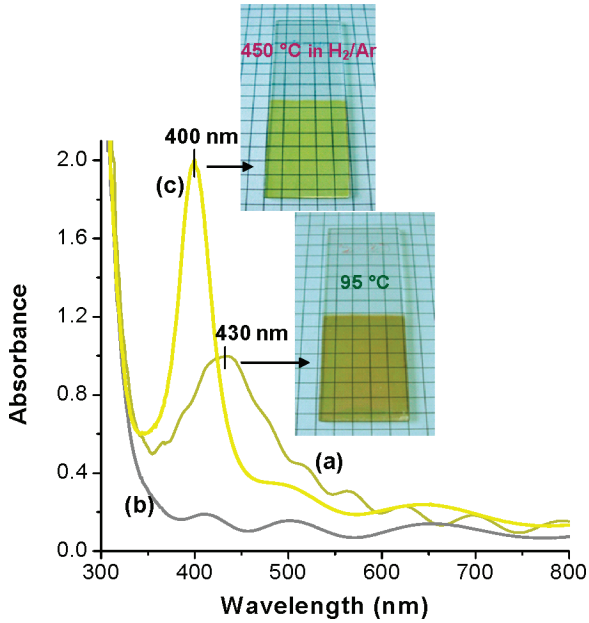

FIGURE 2. UV−visible spectra of Ag−TiO_2 NP codoped SiO_2 films deposited on ZrO_2 barrier-coated soda-lime substrates after different drying and heat-treatment stages: (a) 95 °C (1.5 h), (b) 450 °C in air (1 h), and (c) 450 °C in H_2/Ar (1 h). Inset shows photos of the dried (95 °C) and final heat-treated (450 °C in H_2/Ar) films.

self-lock poly bags) for several months without any change in color or spectral property.

3.2. UV−Visible Spectral Studies. The 95 °C dried Ag−TiO_2 codoped films showed a relatively broad peak at about 430 nm (Figure 2a) due to the surface plasmon resonance (SPR) of the embedded Ag NPs (see also the photo of film in the inset of Figure 2). The same film when air-heated at 450 °C became hard but lost the yellow color because of the oxidation of silver to silver oxide, and as a consequence the SPR peak disappeared completely (Figure 2b) (26). This transparent and colorless film when reheated to 450 °C under a H_2/Ar atmosphere for 1 h became bright yellow and showed sharper peak at around 400 nm (Figure 2c) with increase in peak intensity (about 2 times compared to the 95 °C dried films). The photo of this film is also presented in the inset of Figure 2. The reappearance of the Ag−SPR peak confirmed the reduction of silver oxide to Ag NPs in the presence of H_2 (reducing atmosphere) and heat. The sharper appearance with blue shifting of the SPR absorption is primarily due to the increase in electron concentration on Ag NPs captured during the heat-treatment in reducing (H_2) atmosphere (26). The bright yellow color of the films seemed to be stable, as the absorption values at the 400 nm plasmon band remained almost unchanged after keeping the films under fluorescent light up to 45 days. For a comparative study, Ag NP incorporated SiO_2 films were also prepared on ZrO_2 barrier-coated substrates and annealed in a fashion similar to that of Ag−TiO_2 codoped films. The Ag-incorporated SiO_2 films (without TiO_2) also appeared yellow in color, showing a broad absorption peak at about 421 nm after drying at 95 °C. This film also became colorless after air annealing at 450 °C (see Figure S1 in the Supporting Information) because of the oxidation of Ag NPs. On further heat-treatment in H_2/Ar, this film again transformed to yellow showing a sharper Ag−SPR peak at ∼401 nm (see Figure S1 in the Supporting Information).

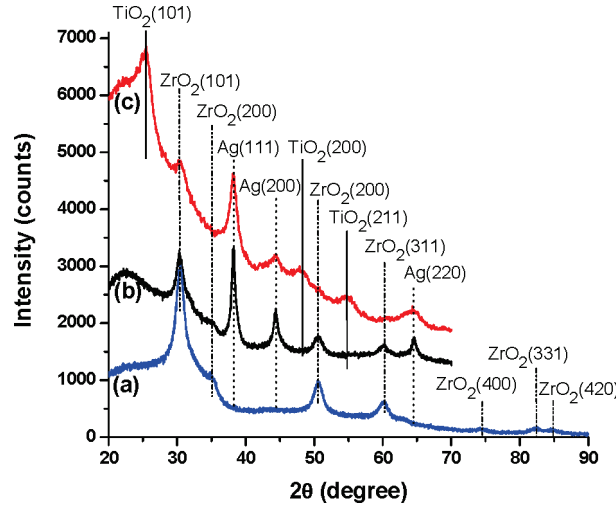

FIGURE 3. GIXRD patterns of the films deposited on soda-lime glass substrates: (a) ZrO_2 barrier coating heat-treated at 500 °C in air, (b) Ag-doped SiO_2 and (c) Ag-TiO_2 codoped SiO_2 films deposited on ZrO_2 barrier-coated substrates. In b and c, final heat-treated (450 °C in H_2/Ar for 1 h) films were used.

3.3. X-ray Diffraction Studies of the Films. GIXRD study of the heat-treated films was undertaken to identify different crystalline phases present in the films and the results are presented in Figure 3. As shown in Figure 3a, the ZrO_2 barrier film has a crystalline feature which matched with the cubic ZrO_2 (2θ = 30.2, 52, and 60°; JCPDS #00−42−1164) phase. The Ag incorporated SiO_2 films heat-treated at 450 °C in H_2/Ar showed Bragg reflections corresponding to ZrO_2 (originating from the barrier layer), and Ag NPs embedded in the SiO_2 films. The Ag−TiO_2 codoped SiO_2 films also showed crystalline ZrO_2 reflections, as well as peaks corresponding to the anatase TiO_2 (2θ = 25, 48, and 54°; JCPDS #00−42−1164) and Ag NPs (2θ = 38.11, 44.27, and 64.42°; JCPDS #00−04−0783). Silica remained amorphous because no peaks corresponding to crystalline silica was observed.

3.4. FESEM Study. The surface of the film was cleaned with absolute ethanol soaked tissue paper and subjected to FESEM study. As shown in the Figure 4a, uniformly distributed Ag NPs of average size ∼6 nm can be observed through out the film. The size distribution of Ag NPs obtained from the FESEM image is presented in Figure 4b. These NPs were embedded inside the films but expected to exist close to the surface. Although anatase TiO_2 NPs of average size 15 nm were incorporated into the silica matrix, FESEM did not show any discrete TiO_2 NPs. It seemed TiO_2 and SiO_2 mixed well and formed a homogeneous film matrix.

3.5. TEM Studies. TEM analysis of the Ag−TiO_2 NPs codoped film is presented in Figure 5. The cleaned film was scratched off from the substrates carefully to avoid contamination of the barrier ZrO_2, and deposited on a carbon-coated Cu grid for TEM study. The TEM bright field image (Figure 5a) showed existence of spherical Ag NPs with darker appearance in the porous film matrix. The corresponding EDX analysis (Figure 5b) showed the presence of Si, Ti, Ag,

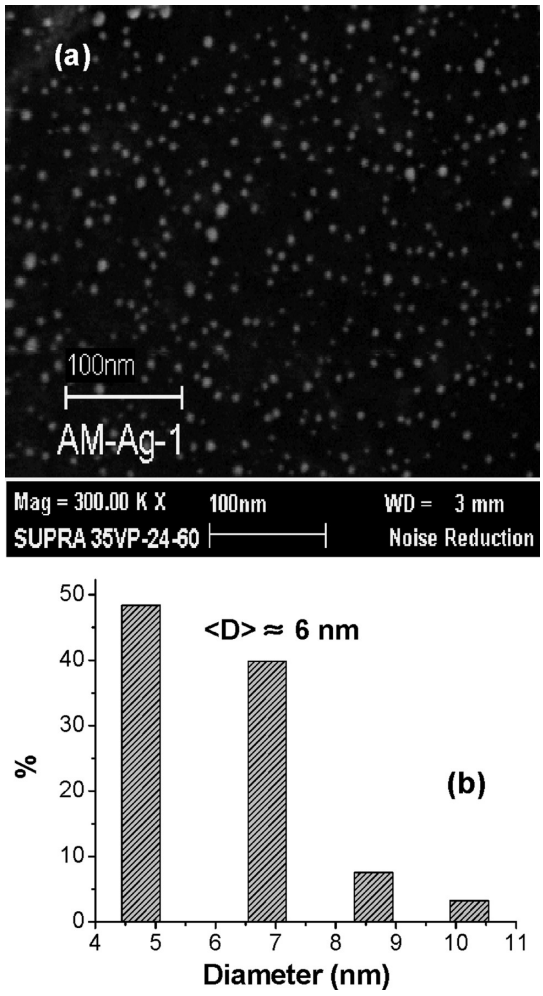

FIGURE 4. (a) FESEM image showing the top surface of the final heat-treated (450 °C in H_2/Ar) Ag−TiO_2 codoped SiO_2 film deposited on ZrO_2 barrier-coated soda-lime substrate and (b) histogram showing the size distribution of Ag NPs.

and O from the film sample, whereas C and Cu peaks were from carbon-coated Cu grid. Absence of Zr peaks confirmed that the analyzed film was not contaminated with the barrier layer ZrO_2. TEM-EDX quantitative analysis showed the presence of Ag with mol ratios ~2.5 part to 97.5 part (SiO_2 + TiO_2). This was lower than the nominal concentration of Ag (5 mol %) added to the sol. However, it may be noteworthy that the amount of Ag found in this study is much higher than the previously reported work where 10 mol % Ag was added to the TiO_2 but less than 1 mol % was found to be present in the film (20). The average size distribution (Figure 5c) of the embedded Ag NPs was (176 particles were measured from different bright field TEM images) estimated to be ~6.9 nm. This value is quite close to the average size of Ag NPs measured from the FESEM image. The selected area electron diffraction (SAED) pattern presented in Figure 5d showed the lines corresponding to fcc Ag and anatase TiO_2. The bright field TEM image (Figure 5a) also showed no distinct TiO_2 NPs in the films. However, the high-resolution image (Figure 5e) obtained from the marked area of Figure 5a (shown as square box and arrow) showed existence of distinct fringe patterns corresponding to the (101) crystalline plane of anatase TiO_2. The fringe pattern of the spherical particle (with darker appearance) matched well with the Ag (111) lattice plane (Figure 5e). So the TEM study confirmed that the anatase TiO_2 were present with the SiO_2 forming a relatively porous film matrix embedded with spherical Ag NPs.

We incorporated 5 mol % Ag with respect to the total equivalent amount of oxide (TiO_2 + SiO_2) content in the sol. However, TEM-EDX analysis of the film showed presence of about 2.5 mol % Ag in the film. Although a ZrO_2 barrier layer was applied on the soda-lime glass to resist the diffusion of Ag into the substrate, however, no control of diffusion toward the upper surface was possible. FESEM image obtained from the cleaned film surface showed the presence of uniform Ag NPs throughout the film and it seemed that the embedded NPs were present close to the surface of the films. These results suggested that the Ag ions migrated toward the surface during the air annealing stages (oxidation of Ag to Ag^+), and some amount was possibly escaped out from the top surface of the films.

3.6. Antibacterial Activity. From the FESEM and TEM studies we observed the presence of Ag NPs of average size 6−7 nm, and this size range should show better bacterial growth inhibition (1, 27). We have studied the time dependence of the bacterial growth in the presence of different coated films, and Figure 6 shows the representative time points at 0, 2, and 8 h. We observed that after 8 h of incubation there was almost no bacterial growth in the case of Ag−TiO_2 NPs codoped film (Figure 6a), whereas some growth was observed on Ag-doped film (Figure 6b). In the case of control sample (bare glass) significant growth of bacteria was observed even after 2 h of incubation (Figure 6c). In a separate experiment, plates were incubated for longer time (24 h) and their photographs are presented in Figure 7. In this case, a TiO_2−SiO_2 (without Ag) film was also incubated. In this set, practically no growth of the bacterial colonies was observed on the sample plate of Ag−TiO_2 NPs codoped film (Figure 7a), whereas few colonies on the sample plate of Ag-doped film (Figure 7b) were observed. As expected, there was a good amount of bacterial growth in plates of TiO_2−SiO_2 (without Ag) (Figure 7c) and lots of growth in the case of control sample (bare glass) (Figure 7d). Considering the growth pattern in the case of bare glass (control sample; Figures 6c and 7d) as the normal and spontaneous growth of *E. coli*, it can be assumed that the sample plate in Figures 6a and 7a (Ag−TiO_2 NPs codoped film) showed very good bacterial growth inhibiting ability. We tested the antibacterial activity with the Ag-doped SiO_2 film (sample plates shown in Figures 6b and 7b) to check whether the presence of TiO_2 NPs in the film could boost the antibacterial activity of Ag particles. In fact, we found that the Ag−TiO_2 codoped SiO_2 film showed relatively better growth inhibition of *E. coli* (Figures 6a and 7a) compared to the Ag-doped SiO_2 film (Figures 6b and 7b) upon contact with the surface under regular light. In another word, although there was no exposure of any samples to the UV light during the experimental procedures, the presence of anatase TiO_2 NPs enhanced the overall antibacterial activity

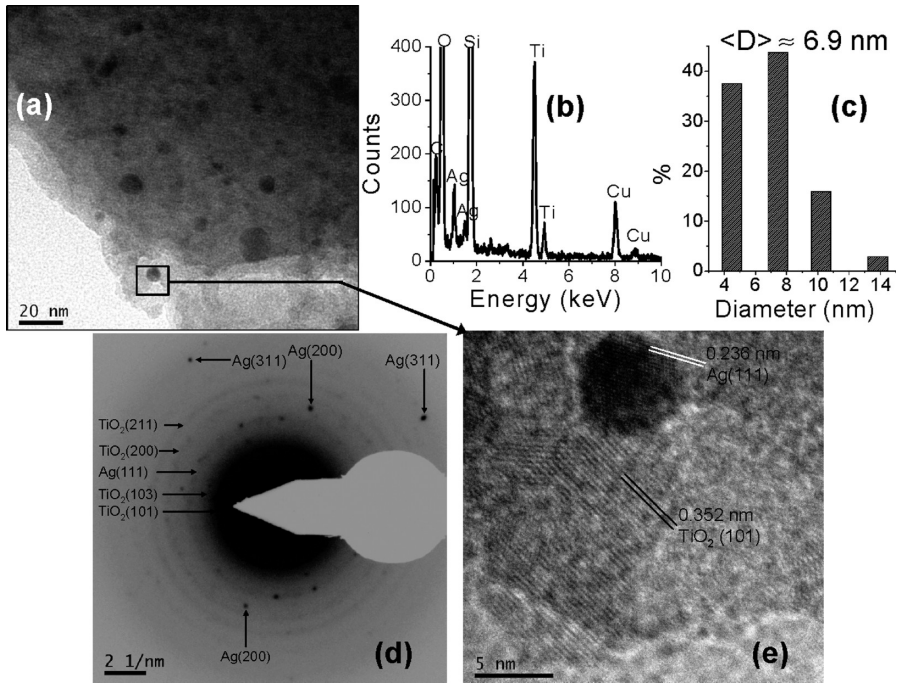

FIGURE 5. TEM studies of the final heat-treated (450 °C in H_2/Ar) Ag—TiO_2 codoped SiO_2 films deposited on ZrO_2 barrier-coated soda-lime substrate: (a) bright-field image, (b) EDX pattern showing the existence of different elements present in the film (C and Cu are from the carbon-coated copper grid used for the TEM study), (c) overall size distribution of embedded Ag NPs, (d) SAED pattern obtained from image a, and (e) HRTEM image of the marked area of image a.

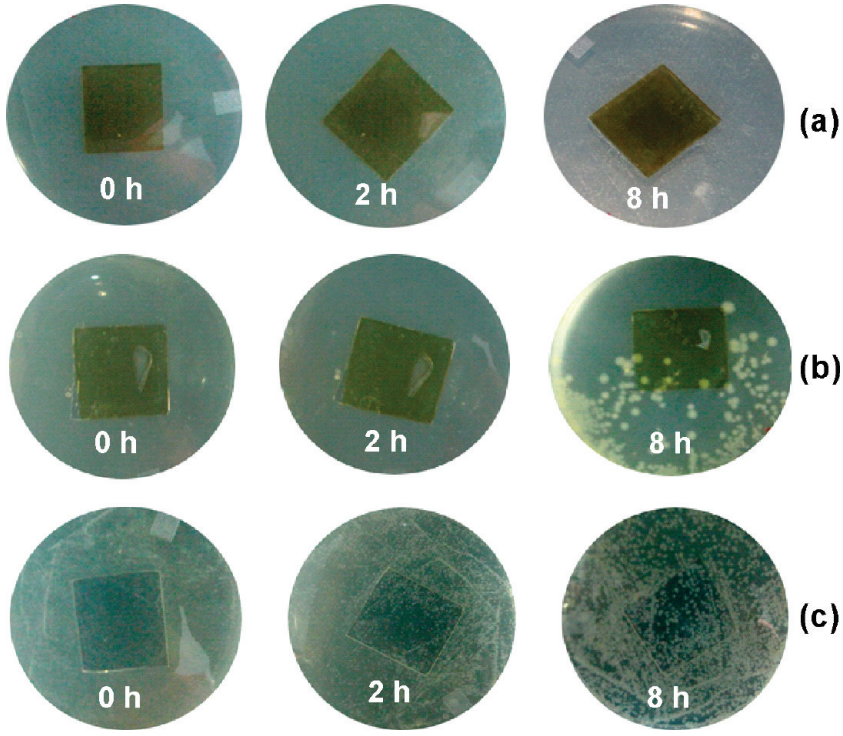

FIGURE 6. Visual images of bacterial growth with respect to time (indicated in the respective images): (a) Ag—TiO_2 NP codoped SiO_2 and (b) Ag-doped SiO_2 films, and (c) control (bare glass). Films were deposited on ZrO_2 barrier-coated glasses and heat-treated at the respective final temperatures.

of Ag NPs (22, 24, 25). We incorporated high amount of TiO_2 NPs in the film matrix. In the porous film matrix the TiO_2 NPs remained well mixed with the SiO_2, and it can be expected that the light easily comes into the contact with TiO_2 NPs. It is known that the ordinary solar radiation containing 3—5% UV light can excite (e^-—h^+) this high amount of anatase TiO_2 NPs to some extent. These excited electrons can be trapped by Ag, which will stabilize its metallic state and expected to enhance the antibacterial activity through free radical mechanism. As the Ag NPs were populated close to the surface of the film (as observed by FESEM study), the antibacterial activity is expected to be

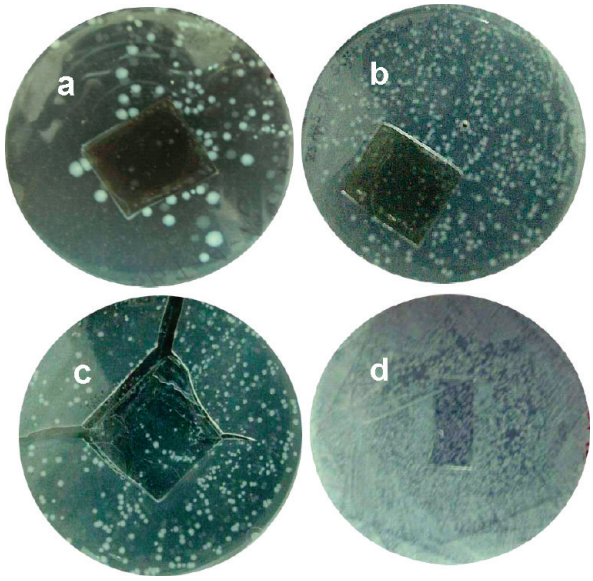

FIGURE 7. Visual images of bacterial growth after 24 h of incubation: (a) Ag−TiO_2 NP codoped SiO_2, (b) Ag-doped SiO_2, and (c) TiO_2 NP incorporated SiO_2 (TiO_2−SiO_2) films, and (d) control (bare glass). Films were deposited on ZrO_2 barrier-coated glasses and heat-treated at the respective final temperatures.

enhanced through contact. Further, due to the trapping of electrons by the Ag NPs, the e^-−h^+ recombination was prevented (28) and hence the h^+ containing TiO_2 would also help to enhance the antibacterial activity. Both these effects may be supportive of such enhancement of antibacterial property of the Ag−TiO_2 codoped film. A significant bacterial growth was observed on the plate of TiO_2−SiO_2 film without Ag (Figure 7c). So TiO_2 NPs without Ag showed no such bacterial growth inhibiting property.

4. CONCLUSION

In this work we demonstrated a synthetic protocol to develop Ag-TiO_2 NPs codoped SiO_2 films on crystalline ZrO_2 barrier-coated soda-lime glass substrates. The films were scratch-resistant, transparent, bright yellow in color, relatively porous yet hard enough for any practical applications. This Ag−TiO_2 combined NPs embedded SiO_2 film was found to be stable in ordinary light for prolonged period of time and exhibited good growth inhibition just upon contact with the gram-negative bacteria *E. coli*. Such coatings can be deposited on glass or similar substrates which are commonly used in various furnishing, surgical and community areas of hospital. The presence of anatase TiO_2 with Ag helped in stabilizing the metallic Ag NPs and improving the overall antibacterial activity.

Acknowledgment. Financial support from the Department of Science and Technology (DST), Government of India, under National Nano Mission programme is thankfully acknowledged. A.M. and S.B. thank CSIR for awarding a Research Associateship and Junior Research Fellowship, respectively.

Supporting Information Available: Optical spectra of Ag-doped SiO_2 films deposited on ZrO_2 barrier-coated soda-lime substrates treated under different conditions. This material is available free of charge via the Internet at http://pubs.acs.org.

REFERENCES AND NOTES

(1) Morones, J. R.; Elechiguerra, J. L.; Camacho, A.; Holt, K.; Kouri, J. B.; Ramirez, J. T.; Yacaman, M. J. *Nanotechnology* **2005**, *16*, 2346–2353.
(2) Chen, X.; Zheng, Z.; Ke, X.; Jaatinen, E.; Xie, T.; Wang, D.; Guo, C.; Zhao, J.; Zhu, H. *Green Chem.* **2010**, *12*, 414–419.
(3) Zhang, H.; Chen, G. *Environ. Sci. Technol.* **2009**, *43*, 2905–2910.
(4) Panacek, A.; Kvitek, L.; Prucek, R.; Kolar, M.; Vecerova, R.; Pizurova, N.; Sharma, V. K.; Nevecna, T.; Zboril, R. *J. Phys. Chem. B* **2006**, *110*, 16248–16253.
(5) Sondi, I.; Salopek-Sondi, B. *J. Colloid Interface Sci.* **2004**, *275*, 177–182.
(6) Kim, S. K.; Kuk, E.; Yu, K. N.; Kim, J. H.; Park, S. J.; Lee, H. J.; Kim, S. H.; Park, Y. K.; Park, Y. H.; Hawang, C. Y.; Kim, Y. K.; Lee, Y. S.; Jeong, D. H.; Cho, M. H. *Nanomed. Nanotechnol. Biol. Med.* **2007**, *3*, 95–101.
(7) Jain, P.; Pradeep, T. *Biotechnol. Bioeng.* **2005**, *90*, 59–63.
(8) Rattanawaleedirojn, P.; Saengkiettiyut, K.; Sangsuk, S. *Nanotechnology* **2008**, *7*, 75–79.
(9) Guin, D.; Manorama, S. V.; Latha, J. N. L.; Singh, S. *J. Phys. Chem. C* **2007**, *111*, 13393–13397.
(10) Galya, T.; Sedlarík, V.; Kuritka, I.; Novotny, R.; Sedlaríková, J.; Sáha, P. *J. Appl. Polym. Sci.* **2008**, *110*, 3178–3185.
(11) Egger, S.; Lehmann, R. P.; Height, M. J.; Loessner, M. J.; Schuppler, M. *Appl. Environ. Microbiol.* **2009**, *75*, 2973–2976.
(12) Saint, S.; Elmore, J. G.; Sullivan, S. D.; Emmerson, S. S.; Koepsell, T. D. *Am. J. Med.* **1998**, *105*, 236–241.
(13) De, S.; De, G. *J. Mater. Chem.* **2006**, *16*, 3193–3198.
(14) Medda, S. K.; De, G. *Ind. Eng. Chem. Res.* **2009**, *48*, 4326–4333.
(15) De, G.; Licciulli, A.; Massaro, C.; Tapfer, L.; Catalano, M.; Battaglin, G.; Meneghini, C.; Mazzoldi, P. *J. Non-Cryst. Solids* **1996**, *194*, 225–234.
(16) Secondary ion mass spectrometry (SIMS) depth profile studies of the heat-treated (300−400 °C) Ag-doped SiO_2 sol-gel films (thickness ~0.15 μm) deposited on soda-lime glass substrate showed diffusion of large amount of Ag inside the glass up to the depth of >2.5 μm. G. De et al., unpublished results.
(17) Chen, S.; Akai, T.; Kadono, K.; Yazawa, T. *Appl. Phys. Lett.* **2001**, *79*, 3687–3689.
(18) Borsella, E.; Battaglin, G.; Garcia, M. A.; Gonella, E.; Mazzoldi, P.; Polloni, R.; Quaranta, A. *Appl. Phys. A: Mater. Sci. Process.* **2000**, *71*, 125–132.
(19) De, G. *J. Sol−Gel Sci. Technol.* **1998**, *11*, 289–298.
(20) Jeon, H.-J.; Yi, S.-C.; Oh, S.-G. *Biomaterials* **2003**, *24*, 4921–4928.
(21) Page, K.; Palgrave, R. G.; Parkin, I. V.; Wilson, M.; Savin, S. P.; Chadwick, A. V. *J. Mater. Chem.* **2007**, *17*, 95–104.
(22) Shah, Md. A. S.; Nag, M.; Kalagara, T.; Singh, S.; Manorama, S. V. *Chem. Mater.* **2008**, *20*, 2455–2460.
(23) Carturan, G.; Mea, G. D.; Paccagnella, A.; Soraru, G. D.; Rizzo, C. *J. Non-Cryst. Solids* **1989**, *111*, 91–97.
(24) Wu, T.-S.; Wang, K.-X.; Li, G.-D.; Sun, S.-Y.; Sun, J.; Chen, J.-S. *ACS Appl. Mater. Interface* **2010**, *2*, 554–550.
(25) Chen, S. F.; Li, J. P.; Qian, K.; Xu, W. P.; Lu, Y.; Huang, W. X.; Yu, S. H. *Nano Res.* **2010**, *3*, 244–255.
(26) Pal, S.; De, G. *Mater. Res. Bull.* **2009**, *44*, 355–359.
(27) Pal, S.; Kyung Tak, Y.; Song, M. J. *Appl. Environ. Microbiol.* **2007**, *73*, 1712–1720.
(28) Stathatos, E.; Petrova, T.; Lianos, P. *Langmuir* **2001**, *17*, 5025–5030.

AM100363D